

Topology of $SU(N)$ gauge theories at $T \simeq 0$ and $T \simeq T_c$

Biagio Lucini^{a,b}, Michael Teper^a and Urs Wenger^{a,c}

^aTheoretical Physics, University of Oxford,
1 Keble Road, Oxford OX1 3NP, U.K.

^bInstitute for Theoretical Physics, ETH Zürich,
CH-8093 Zürich, Switzerland

^cNIC/DESY Zeuthen, Platanenallee 6, 15738 Zeuthen, Germany

Abstract

We calculate the topological charge density of $SU(N)$ lattice gauge fields for values of N up to $N = 8$. Our $T \simeq 0$ topological susceptibility appears to approach a finite non-zero limit at $N = \infty$ that is consistent with earlier extrapolations from smaller values of N . Near the deconfining temperature T_c , we are able to investigate separately the confined and deconfined phases, since the transition is quite strongly first order. We find that the topological susceptibility of the confined phase is always very similar to that at $T = 0$. By contrast, in the deconfined vacuum at larger N there are no topological fluctuations except for rare, isolated and small instantons. This shows that as $N \rightarrow \infty$ the large- T suppression of large instantons and the large- N suppression of small instantons overlap, even at $T \simeq T_c$, so as to suppress *all* topological fluctuations in the deconfined phase. In the confined phase by contrast, the size distribution is much the same at all T , becoming more peaked as N grows, suggesting that $D(\rho) \propto \delta(\rho - \rho_c)$ at $N = \infty$, with $\rho_c \sim 1/T_c$.

1 Introduction

The finite-temperature deconfinement transition of $SU(N)$ gauge theories has, recently, been studied numerically for gauge groups ranging from $N = 2$ to $N = 8$ [1, 2]. The transition is first order for $N \geq 3$ and, as with much of the other physics of these gauge theories [3], the approach to the $N = \infty$ limit appears to be rapid.

As part of this ongoing study [4] we have investigated the topological properties of the gauge fields in the neighbourhood of the transition. Since for $N \geq 4$ the transition is quite strongly first order, it is possible to do this for the confined and deconfined phases separately, at exactly the same temperature, when $T \simeq T_c$. What happens as $N \rightarrow \infty$ is of particular interest and what we find is that the topological properties in the confined phase are the same for all T as at $T = 0$, while in the deconfined phase there are no topological fluctuations at all, even at $T \simeq T_c$. Since at $N = \infty$ QCD (with $m_q > 0$) and quenched QCD are the same, this conclusion also applies to the deconfined phase of $\text{QCD}_{N=\infty}$. Moreover, as we shall see, the suppression of topological fluctuations in the deconfined phase, and the corresponding restoration of the $U_A(1)$ symmetry, is very rapid in N (probably exponential).

We have also performed some $SU(6)$ and $SU(8)$ calculations at $T = 0$ in order to obtain the string tension, σ , which then provides a scale in which to express the calculated values of the deconfining temperature T_c . We have, at the same time, calculated the topological charge and this allows us to extend earlier $T = 0$ calculations, both of the topological susceptibility [3, 5] and of the size distribution of the topological charges [3, 6]. This size distribution becomes narrower as N increases suggesting that it might be tending to a simple δ -function.

2 Some expectations at large N

We review here some expectations that one has about topology in the large- N limit, that follow from general counting arguments [7].

2.1 The topological susceptibility

The topological susceptibility is defined as $\chi_t \equiv \langle Q^2 \rangle / V$, where V is the volume of space-time and Q is the total topological charge. Since fluctuations are suppressed as $N \rightarrow \infty$, so that one can imagine $N = \infty$ physics being given by a single (gauge-invariant) Master Field [8], and since $\langle Q^2 \rangle$ is a measure of fluctuations, the leading-order value of χ_t should vanish and one needs to ask at what order in $1/N$ one expects it to appear.

We can write

$$\langle Q^2 \rangle = \sum_{x,y} \langle Q(x)Q(y) \rangle = V \sum_x \langle Q(x)Q(0) \rangle \quad (1)$$

and we expect $\langle Q(x)Q(y) \rangle$ to factorise up to relative corrections of $O(1/N^2)$

$$\langle Q(x)Q(0) \rangle \stackrel{N \rightarrow \infty}{\cong} \langle Q(x) \rangle \langle Q(0) \rangle + f(x)O(N^{\zeta-2}) = \langle Q(0) \rangle^2 + f(x)O(N^{\zeta-2}) \quad (2)$$

where we take the N -dependence of the leading factorised term to be N^ζ , and we use the fact that $\langle Q(x) \rangle = \langle Q(0) \rangle$ by translation invariance. Putting this together and using $\langle Q(0) \rangle = \langle Q \rangle/V$ we obtain

$$\frac{\langle Q^2 \rangle}{V} = \sum_x \left\{ \frac{\langle Q \rangle}{V} \right\}^2 + \sum_x f(x) O(N^{\zeta-2}) = \frac{\langle Q \rangle^2}{V} + \sum_x f(x) O(N^{\zeta-2}). \quad (3)$$

In order to determine ζ let us suppose for the moment that we have added a θ -term to the action, i.e. $\delta S = i\theta Q$, and that we are working with a generic nonzero value of θ so that $\langle Q \rangle \neq 0$. We have

$$\langle Q \rangle = -i \frac{d}{d\theta} \ln Z(\theta) = i \frac{d}{d\theta} \epsilon(\theta) V \quad (4)$$

where we have used $Z = \exp -\epsilon V$ where ϵ is the vacuum energy per unit volume. Now we expect from the usual large- N counting arguments [9] that $\epsilon \propto N^2$ and that a smooth large- N limit is reached if one keeps θ/N fixed i.e.

$$\epsilon(\theta) = N^2 h(\theta/N). \quad (5)$$

Plugging this into eqn(4) and using the notation $\psi \equiv \theta/N$, we immediately see that

$$\langle Q \rangle = i \frac{d}{d\theta} \epsilon(\theta) V = NV i \frac{d}{d\psi} h(\psi) \quad (6)$$

i.e. $\langle Q \rangle \propto NV$. Thus $\zeta = 2$ and we see from eqn(3) that for any $\psi \neq 0$

$$\chi_t \equiv \frac{\langle (Q - \langle Q \rangle)^2 \rangle}{V} \propto O(V^0) O(N^0) \quad (7)$$

where we have generalised the definition of χ_t to allow for $\langle Q \rangle \neq 0$. In obtaining eqn(7) we use the fact that $\sum_x f(x) = O(V^0)$ which follows from the fact that the mass of the lightest glueball with the quantum numbers of $Q(x)$, i.e. $J^{PC} = 0^{-+}$, is non-zero. By continuity we expect that at $\theta = 0$ eqn(7) will be valid and that $\chi_t \propto O(N^0)$.

We therefore expect that χ_t should have a finite non-zero limit as $N \rightarrow \infty$, even though this is really an $O(1/N^2)$ correction in that limit. This is of course nothing but the conventional expectation, needed to explain the mass of the η' [10, 11]. Lattice calculations [3, 5] support this expectation and we shall provide further evidence in this paper.

2.2 The topological charge

We have noted above that for $\theta \neq 0$ we have

$$\frac{\langle Q \rangle}{V} \propto N. \quad (8)$$

This is not unexpected: instantons are $SU(2)$ objects and (in the semiclassical limit) can be simultaneously placed in any of the $\sim N/2$ non-overlapping subgroups of $SU(N)$ without

interacting – even if they are centered at the same point in space-time. At $\theta = 0$, where we work, one continues to expect $O(N)$ charges in every finite region of space-time, although now they will largely cancel in $\langle Q \rangle$. Since the general arguments given in Section 2.1 imply that $\langle Q^2 \rangle \propto N^0$ rather than $\propto N^1$, this cancellation is clearly much stronger than the usual ‘random walk’ of a dilute gas.

There are detailed variational treatments of the instanton partition function that explicitly show how this cancellation can happen [12, 13]. It is instructive to sketch the core of the argument. Since the (anti)instantons can be thrown into $\propto N$ $SU(2)$ subgroups in the space-time volume V , we can expect their numbers to be $n_+, n_- \propto VN$ and equal on the average. That is to say $n_+ + n_- \propto N$ (we drop the ubiquitous factor of V from now on) while the distribution in $Q = n_+ - n_-$ is flat for $Q \ll \sqrt{N}$. (It is easy to see this in an explicit dilute gas calculation.) For the fields not to interact they have to be in subgroups that are exactly orthogonal and this is a set of fields of measure zero. Allowing fluctuations away from these particular subgroups involves interactions. Let γ_s, γ_a label the interactions between like and unlike charges that are in the same volume of space-time. The simplest instanton calculation [12] tells us that the interaction is repulsive with $\gamma_{a,s} \propto 1/N$. Thus the extra interaction piece in the action will be

$$\delta S_{int} \propto \frac{1}{2} \gamma_s n_+ (n_+ - 1) + \frac{1}{2} \gamma_s n_- (n_- - 1) + \gamma_a n_- n_+ \quad (9)$$

which we can rewrite as

$$\delta S_{int} \propto \frac{1}{2} \frac{1+r}{2} \gamma_s (n_+ + n_-)^2 + \frac{1}{2} \frac{1-r}{2} \gamma_s (n_+ - n_-)^2 \quad (10)$$

defining $r = \gamma_a/\gamma_s$ (and suppressing a non-leading term linear in $n_+ + n_-$). The second term provides a factor in the partition function of $\propto \exp -cQ^2$ where $c = O(1)$ since the factor of $1/N$ from γ_s will combine with the usual $1/g^2$ factor to give the ‘t Hooft coupling that is kept constant as $N \rightarrow \infty$. Of course, for $c > 0$ we must assume that $r < 1$ i.e. $\gamma_a < \gamma_s$, since otherwise the favoured configuration would clearly have charges of the same sign, so cancellations would be suppressed and we would have $Q \propto N$. If all this is the case then, given that the partition function is otherwise flat in $Q = n_+ - n_-$ for $Q \ll \sqrt{N}$, this factor of $\exp -cQ^2$ will ensure that $\langle Q^2 \rangle$ is $O(1)$ rather than $O(N)$. What happens to the term $\propto (n_+ + n_-)^2$ in eqn(10) is more difficult to see, and requires the full apparatus of a variational treatment [12]. But the suppression of $\langle Q^2 \rangle$ from $O(N)$ to $O(1)$ is (in this instanton picture) simply the result of the fact that it induces a suppression in the action that is quadratic in Q because it is quadratic in the n_+, n_- . This might appear to be a severe breakdown of the dilute gas approximation, but it occurs within the same region of space-time, and still leaves open the possibility that a dilute gas/liquid picture can describe the interactions of the net charges that are located in different regions of space-time.

It would clearly be interesting to confirm the above expectation, and to explore how it works in the full non-perturbative vacuum of the gauge theory. Unfortunately our lattice calculations were not specifically designed to address this issue. Nonetheless we do calculate two potentially relevant quantities: the total action and $Q_{mod} \equiv \sum_x |Q(x)|$ as a function of

cooling. If there are $O(N)$ topological charges in every region of space-time, and if there is some scatter in the positions and sizes of these charges, then this might be revealed in a component of these two quantities that grows with N . Unfortunately our calculations of Q_{mod} have shown nothing significant (which may be due to the coarseness of our lattice spacing) and while the average plaquette after a given number of ‘cooling sweeps’ (see Section 3) is roughly independent of N , so that the normalised action is $\propto N^2$ (recall the factor $\beta = 2N/g^2 = 2N^2/(g^2N)$ in the lattice action – see Section 3 – and that we keep g^2N fixed as $N \rightarrow \infty$), this is difficult to interpret on its own since we of course expect the full action to show this behaviour irrespective of topological considerations.

2.3 Small instantons at all T

For large N , instantons are exponentially suppressed in N [14]:

$$D(\rho) \propto e^{-S_I} \propto e^{-\frac{8\pi^2}{g^2(\rho)}} = e^{-\frac{8\pi^2}{\lambda(\rho)}N} \quad (11)$$

where S_I is the instanton action, ρ is the instanton size and $\lambda \equiv g^2N$ is the ’t Hooft coupling which is kept constant as $N \rightarrow \infty$. This simple semiclassical argument is incomplete (see e.g. [15, 16, 13]) but is essentially correct for topological charges that are small enough and using the one-loop expression for $g^2(\rho)$ we expect that

$$D(\rho) \propto e^{-S_I} \propto \rho^{\frac{11N}{3}-5}. \quad (12)$$

Thus we expect that there is some critical size ρ_c such that

$$D(\rho) \xrightarrow{N \rightarrow \infty} 0 \quad ; \quad \forall \rho < \rho_c. \quad (13)$$

There is some evidence for this from earlier lattice calculations [3].

This has an important practical consequence for lattice calculations. Since the lattice Monte Carlo is a local process, in that the elementary step consists of changing one link matrix at a time, the value of Q can only change in a sequence of Monte Carlo generated gauge fields if an instanton gradually shrinks until it disappears within a lattice hypercube (or the converse process). For small lattice spacings this requires the presence of lattice fields containing an instanton of size $a \ll \rho \ll \rho_c$. From eqn(13) the probability of such a lattice field $\rightarrow 0$ exponentially fast in N as $N \rightarrow \infty$. Thus at fixed a topology suffers a critical slowing down in N , i.e. the value of Q ceases to change and we cannot calculate $\langle Q^2 \rangle$ in the usual fashion. (Of course, fluctuations corresponding to topological charges of opposite sign can still appear and disappear and in principle one could calculate $\langle Q^2 \rangle$ from the charge Q within a large sub-volume of a very much larger space-time volume – with the latter chosen large enough that the constraint of a fixed total topological charge is negligible.) In practice this means that in our $SU(8)$ calculations, the value of Q ceases to change as we reduce a and we are unable to perform a continuum extrapolation for the susceptibility. Instead we will perform a comparison of the susceptibility at a fixed not-too-small value of a .

2.4 Large instantons at high T

At high T , chromo-electric fields are screened on a scale characterised by the electric screening mass m_{el} . At high enough T the characteristic expansion parameter, $g^2(T)$, is small and it suffices to calculate m_{el} to leading order in perturbation theory, whereupon one finds [17]

$$m_{el}^2(T) = \frac{N}{3}g^2(T)T^2. \quad (14)$$

Here the power of T follows on simple dimensional grounds, and the coupling appears in the familiar combination, g^2N , which is kept constant as $N \rightarrow \infty$. The chromoelectric fields in the core of an instanton are coherent over its size ρ . On the other hand they will necessarily be screened over a distance $O(1/m_{el})$. This means that instantons of size $\rho \gg 1/m_{el} \propto 1/T$ will be strongly suppressed, and we expect the suppression to be a function of ρT . A careful calculation [17] shows that the instanton density, $D(\rho)$, is modified as follows for $\pi\rho T \gg 1$ and $g^2(T) \ll 1$:

$$D(\rho, T) = D(\rho, 0) \exp\left(-\frac{2N}{3}\{\pi\rho T\}^2 - \gamma(\rho T)\right) \quad (15)$$

where $\gamma(\rho T)$ is a weak function of its argument, which we can neglect for our purposes. We note that the dominant suppression in eqn(15) is a function of ρT as expected. It also contains a factor of N , which one would expect for the same reason that it appears in the classical action in eqn(11).

When valid, eqn(15) implies that topological fluctuations on size scales $\rho \gg 1/\pi\sqrt{N}T$ will be heavily suppressed, and that at fixed ρ the suppression will be exponential in N . So what is its domain of validity? The derivation of electric screening requires that we be in the deconfined phase and the leading-order perturbative calculation is only guaranteed to be valid for $T \gg T_c$. So an interesting question is down to what value of T does this calculation hold? The most extreme and yet most elegant scenario is one in which it is valid at all T in the deconfined phase and that as $N \rightarrow \infty$ the small instanton suppression described in the previous section, overlaps with this larger instanton suppression, so that all topological fluctuations vanish exponentially with N at any value of T , in the deconfined phase. This, as we shall see below, is indeed what appears to happen.

3 The lattice calculation

The lattice calculations have been described in detail elsewhere [1, 2] and the calculation of the topological charge density is precisely as in [3]. We shall therefore restrict ourselves to a minimal description here and refer the interested reader to those earlier papers.

We work on periodic hypercubic lattices. We label the lattice spacing by a and the size, in lattice units, by $L_s^3 L_t$. For L_s sufficiently large this corresponds to the field theory at a finite temperature

$$T = \frac{1}{aL_t}. \quad (16)$$

If $L_s, L_t \gg 1/aT_c$ we refer to the system as being at $T = 0$, although this is of course not exactly the case. The variables are $SU(N)$ matrices assigned to the links of the lattice. We employ the usual plaquette action [3] which contains the factor

$$\beta = \frac{2N}{g^2}. \quad (17)$$

Here g^2 is the bare coupling defined at the cut-off scale a , and by varying the value of β we vary the value of a . If we tune $a \rightarrow 0$ we recover the continuum field theory in Euclidean space-time, if $T = 0$, or the statistical physics of the theory at temperature T , more generally.

We evaluate the lattice Feynman Path Integral/Partition Function using standard Monte Carlo techniques. At a fixed value of β we can calculate the $T = 0$ string tension in lattice units, $a^2(\beta)\sigma$, and its value allows us to express the lattice spacing $a(\beta)$ in physical units. If we increase β on a lattice with $L_s \gg L_t$ we will find a deconfining transition at some $\beta = \beta_c$. The corresponding deconfining temperature is

$$a(\beta_c)T_c = \frac{1}{L_t}. \quad (18)$$

Dividing this by the $T = 0$ value of $a(\beta = \beta_c)\sqrt{\sigma}$ we obtain a value of the dimensionless ratio $T_c/\sqrt{\sigma}$ which differs from the continuum value by lattice corrections of order $a^2(\beta_c)$. For larger N we have typically calculated β_c for $L_t = 5, 6, 8$ and this allows us to make the desired $a \rightarrow 0$ continuum extrapolation.

We calculate the topological charge density using one of the standard methods [3, 18]. For smooth lattice gauge fields one can define a lattice topological charge density $Q_L(x)$ as follows:

$$Q_L(x) = \frac{1}{32\pi^2} \varepsilon_{\mu\nu\rho\sigma} \text{ReTr}\{U_{\mu\nu}(x)U_{\rho\sigma}(x)\} \xrightarrow{a \rightarrow 0} a^4 Q(x) + O(a^6) \quad (19)$$

where $Q(x)$ is the continuum topological charge density. To obtain a smooth lattice field from a rough Monte Carlo generated lattice field we apply an iterative ‘cooling’ procedure [3, 18]. Using eqn(19) on the cooled lattice field we obtain its total topological charge $Q_L = \sum_x Q_L(x)$. This will not be an integer because of the lattice corrections in eqn(19), but can easily be rounded to the appropriate integer. We can also attempt to identify individual instantons by looking for peaks in $Q_L(x)$ and applying the classical continuum relation

$$Q_{peak} = \frac{6}{\pi^2 \rho^4}. \quad (20)$$

to extract the instanton size, ρ , from the peak height. In this way we can calculate an instanton size density, $D(\rho)$.

If we use a modest number of cooling sweeps (typically 10 or 20) the calculated topological charge is accurate except in the presence of very narrow charges whose interpretation is naturally ambiguous on a lattice. One can see this by comparing with a fermionic calculation of Q using fermions that satisfy the index theorem [6]. The topological charge density, on the other hand, is steadily distorted by cooling and so the information one obtains on $D(\rho)$ is less

reliable. (Although here too there is some evidence from using massless fermions as a probe, that the distortions are not large for a small number of cooling sweeps [19].) Together with the crudeness of eqn(20) as a pattern recognition algorithm for a dense ‘instanton’ ensemble (see e.g. [20] for more sophistication) it is clear that our estimate of $D(\rho)$ must be regarded as semi-quantitative. In particular, while small instantons are easy to identify, since the peak is large, very large instantons correspond to very small and smooth peaks which might be remnant artifacts of the cooling procedure. In this paper we will make some progress in dealing with this latter uncertainty.

4 Results

4.1 Topological susceptibility at $T=0$

In our ‘ $T = 0$ ’ $SU(8)$ calculation, it is only for the coarsest lattice spacings that Q changes sufficiently frequently that we obtain a usefully accurate value for $\langle Q^2 \rangle$. This means that we cannot reliably extrapolate the susceptibility to the continuum limit and compare its value with continuum values previously obtained for $N \leq 5$ in [3] and for $N \leq 6$ in [5] as we would ideally wish to do. Instead we will calculate the dimensionless ratio of the susceptibility, $a^4 \chi_t$, and the string tension, $a^2 \sigma$, i.e. $a \chi_t^{1/4} / a \sqrt{\sigma} \equiv \chi_t^{1/4} / \sqrt{\sigma}$, at a fixed value of a , chosen so that we are able to obtain an accurate $SU(8)$ value. We do so for $N = 2, 3, 4, 6, 8$. The large- N counting for the lattice gauge theory is the same as for the continuum gauge theory [21], and so one can perform an extrapolation to $N = \infty$, using corrections that are powers of $1/N^2$.

If we want to use the ‘same’ value of a in different $SU(N)$ gauge theories, we need to measure it in units of some physical quantity that has a smooth large- N limit. We shall choose to fix the value of a in units of the deconfining temperature, T_c . To be precise, the value of a that we choose corresponds to $a = 1/5T_c$. That is to say, we perform our calculations at the value of β at which the gauge theory on an L^35 lattice (with $L \gg 5$) will undergo a deconfining transition. We could have used some other physical quantity, such as the string tension, to fix a and the resulting values of β would have differed, because $T_c/\sqrt{\sigma}$ does vary with N . But because such physical ratios possess a smooth large- N limit, any difference will correspond to an change in the coefficients of terms that are higher order in $1/N^2$.

In Table 1 we list our results for $\langle Q^2 \rangle$ for $N = 2, \dots, 8$. We show the lattice sizes, the string tensions, and the values of β for each value of N . We also show for each N the critical value of β at a lattice spacing $a = 1/5T_c$. We see that the value of β we use is always, within errors, equal to $\beta_c(a = 1/5T_c)$, i.e. the lattice spacing is constant across all N when expressed in units of T_c . At a finite lattice spacing different methods of calculating Q will differ. The value we show is obtained after 20 cooling sweeps. Q_r is the real number obtained directly from summing our twisted plaquette operator, while Q_I has been rounded to the appropriate neighbouring integer value. We show in Table 2 the resulting values of the dimensionless ratio $\chi_t^{1/4}/\sqrt{\sigma}$ that we wish to compare across N .

In Fig. 1 we plot the values of $\chi_t^{1/4}/\sqrt{\sigma}$ against the expected expansion parameter $1/N^2$. To fit the N -dependence we use as few correction terms as possible. However a simple $1/N^2$

correction does not provide an acceptable fit, if we insist on fitting all the way down to $N = 2$ (or even only down to $N = 3$). We therefore introduce an additional $1/N^4$ correction and this enables us to obtain an acceptable fit. In that case our best fits are

$$\frac{\chi_t^{1/4}}{\sqrt{\sigma}} = \begin{cases} 0.397(7) + \frac{0.35(13)}{N^2} - \frac{1.32(41)}{N^4} & \text{using } Q_I, \\ 0.382(7) + \frac{0.30(13)}{N^2} - \frac{1.02(42)}{N^4} & \text{using } Q_r, \end{cases} \quad (21)$$

with a goodness of fit $\chi^2 \simeq 1.0, 1.3$ per degree of freedom respectively. (The difference between the two fits is an $O(a^2)$ lattice correction and should disappear in the continuum limit.) As we see from Fig. 1 the convergence to the $N = \infty$ limit is rapid, and our values are accurate enough, and extend over a large enough range of N , to make this a reasonably compelling conclusion.

As an aside we note that the coefficient of the $1/N^4$ term in eqn(21) is quite large compared to the other coefficients, and one might be tempted to ascribe this to the fact that at this lattice spacing we are very close to the bulk transition [3, 2, 4]. However, although the original $a = 0$ large- N calculations of $\chi_t^{1/4}/\sqrt{\sigma}$ [3] were able to interpolate within errors down to $N = 2$ with just a simple $O(1/N^2)$ correction, and therefore the coefficient of the $O(1/N^4)$ term could not be usefully estimated, there are now much more accurate $a = 0$ calculations [5] from which we can extract the coefficient of the $1/N^4$ term in the continuum limit and we find that it has a similar size to the one we have found at $a = 1/5T_c$, although with the opposite sign.

4.2 Topological fluctuations at $\mathbf{T} \simeq \mathbf{T}_c$

When the deconfining transition is first order, as it is for $N \geq 3$, and when T is sufficiently close to T_c , the system will repeatedly tunnel between confined and deconfined phases. At $T \simeq T_c$ the tunneling probability $\rightarrow 0$ as $V \rightarrow \infty$, and what that means for our Monte Carlo calculation is that for large V we have very long sequences of lattice gauge fields that remain in a single phase. Thus we can calculate the topological charge separately in the confined and deconfined phases when T is near T_c . Indeed there exist calculations of this kind in $SU(3)$ (see [22] for early examples) which show that at $T \simeq T_c$ the topological susceptibility is markedly suppressed in the deconfined phase as compared to the confined phase. In this Section we extend these calculations to $N > 3$ so as to learn what happens as $N \rightarrow \infty$.

In Table 3 we present some results on the value that χ_t takes in the confined and deconfined phases at $T \simeq T_c$, for various values of N . The calculations are at a finite lattice spacing and the value of a is the same for all N when expressed in units of T_c : specifically $aT_c \simeq 5$. We present the susceptibility in the form of the dimensionless ratio χ_t/σ^2 , which possesses a simple interpretation in the limit of a dilute gas of topological charges:

$$\frac{\chi_t}{\sigma^2} \equiv \frac{\langle Q^2 \rangle}{\{aL_s\}^3 aL_t \sigma^2} = \frac{\langle N_I \rangle}{\{aL_s\}^3 aL_t \sigma^2} \quad (22)$$

where N_I is the total number of topological charges in the field on the $L_s^3 L_t$ lattice. Thus the quantity χ_t/σ^2 measures the total number of topological charges per unit (four)volume, where

the volume is measured in units of the confining string tension. (Recall that in $\text{QCD}_{N=3}$, one has $\sqrt{\sigma} \simeq 440\text{MeV} \simeq 0.45\text{fm}$.) This interpretation is of course only exact in the dilute gas limit, which is certainly not valid in the confining phase of the $SU(N)$ gauge theory, although, as we shall see below, it does appear to be the case in the deconfined phase.

Since we are at a finite a , different ways of calculating Q will differ – typically by $O(a^2)$ lattice artifacts. The results we present in the remainder of this sub-section are based on the real-valued topological charge, Q_r , calculated after 20 cooling sweeps. The results one would obtain using the integer value topological charge and/or fewer, say 10, cooling sweeps lead to the same conclusions.

For $SU(8)$ we generated two sequences of 50,000 fields on $12^3 5$ lattices with one starting in the confined phase and one in the deconfined phase, and with the inverse coupling β chosen so that $T = 1/5a(\beta) \simeq T_c$. The spatial volume is large enough that not only are there no phase transitions but there is no sign of even a partial tunneling. (We use the time-like Polyakov loop averaged over the lattice as an order parameter to discriminate phases.) Thus there is no ambiguity in calculating quantities separately in the confined and deconfined phases. For $SU(6)$ we do the same (with sequences of 100,000 fields) on $16^3 5$ lattices, for $SU(4)$ (with sequences of 25,000 fields) on $32^3 5$ lattices and for $SU(3)$ on $32^3 5$ lattices. In the last case the volume is small enough that we observe several tunnelings between the phases, but these are sufficiently well-defined that there is no significant ambiguity in separating the phases from each other. That one can work on smaller volumes as $N \uparrow$ is mainly due to the fact that the surface tension of the bubble separating the confined and deconfined vacua increases with N [2] so that for a given volume V the tunneling probability $\rightarrow 0$ as $N \rightarrow \infty$ at $T = T_c$, and so we have longer sequences of fields in which the system remains in a single phase. Finally we remark that while we have not included $SU(2)$ here, since its transition is second order, one also finds in that case a suppression of χ_t for $T > T_c$ [23].

For comparison we also show in Table 3 the ‘ $T=0$ ’ value of χ_t/σ^2 , as obtained from Table 2 (or a slight extrapolation thereof). Comparing the various values in that Table, we see that χ_t/σ^2 remains approximately constant in the confining phase at all T , but that it is strongly suppressed in the deconfined phase. Moreover the suppression becomes rapidly more severe as N grows. To illustrate this we show in Fig. 2 how the ratio of χ_t in the deconfined phase to its value in the confined phase varies with N at $T = T_c$. It seems quite clear that in the deconfined phase $\chi_t(T = T_c) \rightarrow 0$ as $N \rightarrow \infty$.

In Tables 4 to 7 we list some further calculations, some at higher T . (The values marked by a \star in Tables 3 to 7 have been obtained from sequences of fields containing sufficient tunnelings for there to be some danger that the quoted error is underestimated.) Together with our other calculations, these provide more information on the T dependence of χ_t . As an example, we plot in Fig. 3 the T dependence of χ_t/σ^2 for $SU(6)$. We see that the value of χ_t in the deconfined phase shows a strong temperature dependence, vanishing rapidly as T grows.

We conclude that at $N = \infty$ a rather simple picture emerges,

$$\lim_{N \rightarrow \infty} \frac{\chi_t^{\frac{1}{4}}}{\sqrt{\sigma}} = \begin{cases} 0 & \text{deconfined } \forall T, \\ \text{const}(\neq 0) & \text{confined } \forall T, \end{cases} \quad (23)$$

with the suppression in the deconfined phase being very rapid – probably exponential in a power of N . This shows that the the rapid instanton suppression, for which we have reliable semiclassical arguments only at high- T where $g^2(T)$ is small, in fact occurs at all values of T , even down to $T = T_c$, and indeed for all values of the instanton size ρ . The confined phase, on the other hand, appears to be impervious to the large- ρ suppression, even at $T \simeq T_c$. To make this interpretation convincing, we need to estimate the instanton size distribution, and this we shall now do.

4.3 Instanton size distributions

To obtain information on the instanton size density, $D(\rho)$, we smoothen (‘cool’) the lattice fields, so that our lattice topological charge density operator should approximate the continuum one, and we then locate the peaks in that density, $Q(x)$. We identify each of these with an instanton, whose size ρ is given by eqn(20). (As described in Section 3.) This procedure is clearly unambiguous for small instantons, which correspond to large peaks in $Q(x)$, but becomes increasingly more ambiguous for larger instantons that correspond to very low and smooth bumps in $Q(x)$. To help avoid mere fluctuations in the instanton profile being misinterpreted as extra instantons, we do not count peaks that are within a distance of $2a$ of a larger peak. This algorithm is of course very crude (as emphasised in Section 3) but unfortunately we are not aware of a really reliable alternative. We shall therefore focus on the qualitative features of our calculated size densities.

4.3.1 T=0

The $T = 0$ size density was calculated for $2 \leq N \leq 5$ in [3]. Here we shall extend the comparison to $N = 8$. However none of our lattice spacings is as fine as that used in Fig. 13 of [3] and this means that our comparison will be more affected by lattice spacing artifacts.

We start with the calculations listed in Table 1. In each case we calculated the topological charge density after 20 cooling sweeps and the resulting number densities are shown in Fig. 4. What we plot is the number of charges per 10^4 lattice fields with $a = 1/5T_c$. (If one wishes one can translate the volume into more ‘physical’ units using the listed values of the string tension, $a\sqrt{\sigma}$, and using the real world value of $\sqrt{\sigma} \simeq 440\text{MeV}$.) The histograms are for numbers of instantons in bins of ρ that are of size $\delta\rho = 0.25a$. Each point is placed at the average value of ρ within that bin, rather than in the middle of the bin, which means that the points for different N are slightly shifted (in ρ) with respect to each other.

The value of a is very coarse and this means that the effective cut-off induced by the cooling, which here we can estimate to be at about $\rho \sim 2 - 2.5a$ from the $SU(2)$ density, is uncomfortably close to the typical instanton size. Nonetheless some qualitative features are

clear. First is the steepening of the distribution at small ρ . This is expected theoretically and was already observed up to $N = 5$ in [3]. More interesting, and only becoming apparent from the greater range of N available to us in the present calculation, is that the whole distribution, at both small and large ρ , is becoming much more peaked as N grows. Indeed, if we take the distributions in Fig. 4 seriously, we infer that

$$\lim_{N \rightarrow \infty} D(\rho) = c(N)\delta(\rho - \rho_c) \quad ; \quad \rho_c \sim \frac{1}{T_c}. \quad (24)$$

The main uncertainty is to do with the reliability of our identification of the larger topological charges. However since the size distribution narrows with increasing N , the relevant range of ρ comes closer to the average, and so our calculation should be more reliable at larger N . Some explicit checks showing that our conclusions are robust against the detailed cuts of our algorithm would be useful, but have not been performed in the present calculation. Equally, a systematic finite volume study would be useful. For the case of $SU(3)$ there exist such finite volume studies (e.g. [20]) and for higher N our present study has larger spatial volumes at $T \simeq T_c$, which suggest that finite volume corrections are unimportant.

The integrated number of topological charges also appears to increase with N , as shown in Fig. 5. One might imagine that one is seeing the theoretically expected growth that was discussed in Section 2.2. However one needs to be cautious. The volumes at different N that are used here are only constant if expressed in units of T_c . If instead they are expressed in units of, say, $\sqrt{\sigma}$ most of the variation that we see in Fig. 5 for $N \leq 4$ disappears. This is because the volume goes as the 4'th power of the scale. It is only for $N \geq 6$ that we are close enough to $N = \infty$ for this ambiguity to become negligible.

A study similar to that in Fig. 4 but for a smaller value of a would be very useful. Unfortunately we have only performed such a calculation for $SU(8)$. In Fig. 6 we show the resulting $SU(8)$ instanton size distribution obtained on a 16^4 lattice with $a \simeq 1/8T_c$. To compare with distributions at smaller N we use data on 16^4 lattices obtained in [3]. These are mostly at rather different values of a and we rescale the sizes and volumes to $a \simeq 1/8T_c$ in each case. The resulting distributions are plotted in Fig. 6. The cooling/lattice cut-offs are now far from the typical instanton size, and we have an extended region of ρ in which we can observe the dramatic and expected suppression of small instantons. Again we see a rapid narrowing of the distribution as N grows, consistent with eqn(24). The total number of charges appears to grow with N , but once again there are various reasons for considering this to be a much less robust observation.

4.3.2 $T \geq T_c$

We saw in Section 4.2 how, in the deconfined phase, the fluctuations of Q are rapidly suppressed as N grows. In this section we shall look at the size distribution, $D(\rho)$, in that phase. In doing so we shall continue to use the relation eqn(20) to extract ρ , although for larger instantons at high T the solution changes (becoming periodic), as described in [17]. The reason is that both in theory and in practice such periodic instantons are highly suppressed at larger N .

Before looking at the deconfined phase we briefly look at the instanton density in the confined phase, and compare densities at $T \simeq 0$ and $T = T_c$. We focus on $SU(8)$. The $T = T_c$ calculation has been performed on a $12^3 5$ lattice at $\beta = 43.965$ and is compared in Fig. 7 to the $T \simeq 0$ calculation on a 10^4 lattice at $\beta = 44.0$. In the Figure sizes have been rescaled so that the numbers are per 10^4 volume at $\beta = 44.0$. What we see is that there is no significant difference between the densities at $T \simeq 0$ and at $T \simeq T_c$, just as we saw in Table 3 no significant difference in the susceptibilities. The same pattern appears at other values of N . We conclude that the topological content of the confined phase is very much the same at any value of T .

Turning now to the deconfined phase of the $SU(8)$ theory, we plot in Fig. 8 the size distribution obtained on 500 $12^3 5$ lattice fields that are in the deconfined phase and generated at $\beta = 43.965$, i.e. at $T \simeq T_c$. We see that the distribution is entirely located at very large values of ρ (compare Fig. 7 which is in the confined phase) except for a very few peaks (4 out of about 6000) that lie in the range $\rho \in [2, 3.5]$.

To interpret all this we take these 500 fields and use only the largest positive and negative peaks in each field. We then take separately the 4 configurations with $Q \neq 0$ and the 496 lattice fields with $Q = 0$, and we look in Fig. 9 at the size distributions of the two sets separately. Moreover in the former case we show separately the size distribution from peaks with the same sign as Q and from those with the opposite sign. We see that the latter have large values of ρ , just like the $Q = 0$ fields. The former, by contrast, provide the four values $\in [2, 3.5]$ that we noted in the previous paragraph. The interpretation is clear: real topological charges are narrow while the other very broad charges are nothing but artifacts of the partial cooling and do not correspond to real topological charges at all. Given that the high- T suppression we expect theoretically, $\propto \exp(-\frac{2}{3}N\{\pi\rho T\}^2)$, is more severe at larger ρ , the observed gap in the size distribution makes the interpretation of the very low, broad peaks as artifacts quite compelling; as does the fact that these ‘large charges’ do not contribute anything to the net topological charge Q .

It is interesting to note that for the confined phase on the same lattice at the same T we find 7 charges $\in [2, 3]$ (with none narrower). This represents the tail of the highly suppressed small instantons. What we see in the deconfined phase is consistent with being the same tail. In contrast to the confining phase however, where the suppression rapidly relaxes as ρ increases, here there is a cut-off immediately above $\rho \sim 3.5$. Thus it would appear that the the high- T exponential suppression is already effective down to small sizes $\rho \sim 3.5$ and down to modest temperatures $T \simeq T_c$.

Our results at other N show the same features, although the interpretation is simplest in the case of $SU(8)$ because here the deconfined configurations with $Q \neq 0$ are so rare, so that the $Q = 0$ fields are highly unlikely to contain any instanton-antiinstanton pairs that would complicate the argument and the size distributions. To illustrate this we show in Fig. 10 the $SU(6)$ deconfined instanton size density. It show the same features as we saw in Fig. 8 except that the low- ρ peak is much larger – as we would expect because the small- ρ suppression is more severe for $SU(8)$ than for $SU(6)$. For comparison we show the confined density at T_c in Fig. 11. The total number of peaks for $\rho \leq 3.0$ is roughly the same in both cases showing that what is involved is the suppression of charges with larger ρ . (From the ratios of the

densities in the two Figures one can map out the suppression as a function of ρ .) In Fig. 12 we show the $SU(6)$ version of Fig. 9. Unlike the latter we now have a small low- ρ peak from the $Q = 0$ lattice fields. This is because, as we can see, the number of lattice fields with $Q \neq 0$ is much larger and so there is now a finite probability to have lattice fields with well-separated instanton-antiinstanton pairs. For comparison, we show in Fig. 13 the same plot for the confined phase.

We conclude therefore that in the deconfined phase the severe small- ρ suppression is matched by an even more severe larger ρ suppression which, already for $N = 8$ and even at $T \simeq T_c$, extends down to very small ρ . It seems clear that as $N \rightarrow \infty$ the deconfined phase will lose its topological charges exponentially fast at any given ρ ; and that this will be so for all T in this phase. By contrast the confined phase appears to show no variation with T , even at $T \simeq T_c$. Clearly there the semiclassical prediction is obstructed by the non-perturbative fluctuations. We thus have a rather simple picture of the topological properties of the theory as $N \rightarrow \infty$.

5 Conclusions

As we outlined above, there are various theoretical arguments for the large- N behaviour of topological fluctuations in gauge theories, which it is interesting to test in lattice calculations. One expects the topological susceptibility χ_t to have a finite and non-zero $N \rightarrow \infty$ limit (see Section 2.1), despite the fact that simple arguments (see Section 2.2) suggest that the number of topological charges grows $\propto N$. One expects smaller instantons, up to some critical size, to be completely suppressed as $N \rightarrow \infty$ (see Section 2.3) and, since this is a short distance argument, it should occur at all T . Once the temperature T is high enough for the perturbative evaluation of fluctuations around instantons to be reliable, one also expects instantons to be exponentially suppressed in $N\{\pi\rho T\}^2$ (see Section 2.4).

Compared to earlier calculations, our range of N is larger, and we explore both the T and the N dependence of the topological fluctuations. Since the deconfining phase transition is robustly first order for larger N , we are able to investigate the confined and deconfined phases separately at the same value of $T \simeq T_c$.

Our results on the $T \simeq 0$ topological susceptibility (see Fig. 1) show that the topological susceptibility (albeit at a fixed non-zero value of the lattice spacing) does indeed have a finite and non-zero $N \rightarrow \infty$ limit, as suggested by earlier work. The size distribution shows the expected suppression of small topological charges, not only at $T \simeq 0$ (see Fig. 4 and Fig. 6) but also at non-zero T , in both the confined (see Fig. 7) and the deconfined (see Fig. 8) phases. Within the confined phase there appears to be little if any variation with T , at any T , in the character or density of the topological fluctuations. In addition we find that in this phase the size distribution appears to become more peaked as N grows, suggesting that it becomes $\propto \delta(\rho - \rho_c)$ at $N = \infty$.

In the deconfined phase we find a strong suppression of all topological fluctuations which becomes rapidly more severe with increasing N . (See Fig. 2 and Fig. 8.) We infer that the large- T exponential suppression occurs at all $T > T_c$ at large N , and that it overlaps with the

small- ρ suppression so that all topological fluctuations are suppressed.

The low, broad peaks in the deconfined phase (see Fig. 9) are remnant artifacts of the incomplete cooling. They provide us, for the first time, with a measure of the ‘background’ that such artifacts will contribute to all our other size distributions. Of course, these artifacts will depend to some extent on the content of the fields, which is not the same for the confined and deconfined phases. Nonetheless the fact that these artifacts are at such large values of ρ reassures us that the part of the size distributions that is important to our conclusions about the confined phase (in particular the peaking) is robust.

Our calculations thus support a very simple picture of topological fluctuations in the $N = \infty$ limit. In the deconfined phase these disappear completely for all T and for all ρ . In the confined phase all fluctuations with ρ less than some $\rho_c \sim 1/T_c$ disappear, and there is evidence that the same is true for all $\rho > \rho_c$, so that the size distribution becomes a simple δ -function.

Acknowledgements

Our lattice calculations were carried out on PPARC and EPSRC funded Alpha Compaq workstations in Oxford Theoretical Physics, and on a desktop funded by All Souls College. During the course of this research, UW was supported by a PPARC SPG fellowship, and BL by a EU Marie Skłodowska-Curie postdoctoral fellowship.

References

- [1] B.Lucini, M. Teper and U. Wenger, Phys. Lett. B545 (2002) 197 (hep-lat/0206029).
- [2] B.Lucini, M. Teper and U. Wenger, hep-lat/0307017, hep-lat/0309009, hep-lat/0309170.
- [3] B.Lucini and M. Teper, JHEP 0106 (2001) 050 (hep-lat/0307017).
- [4] B.Lucini, M. Teper and U. Wenger, in progress.
- [5] L. Del Debbio, H. Panagopoulos and E. Vicari, JHEP 0208 (2002) 044 (hep-th/0204125).
- [6] N. Cundy, M. Teper and U. Wenger, Phys. Rev. D66 (2002) 094505 (hep-lat/0203030).
- [7] G. 't Hooft, Nucl. Phys. B72 (1974) 461.
E. Witten, Nucl. Phys. B160 (1979) 57.
S. Coleman, 1979 Erice Lectures.
A. Manohar, 1997 Les Houches Lectures, hep-ph/9802419.
S.R. Das, Rev. Mod. Phys. 59(1987)235.
Y. Makeenko, hep-th/0001047.
- [8] E. Witten, in: “Recent Developments in Gauge Theories”, Ed. G. 't Hooft et al. (Plenum Press, 1980).

- [9] E. Witten, Phys. Rev. Lett. 81 (1998) 2862 (hep-th/9807109).
- [10] G. 't Hooft, Physics Reports 142 (1986) 357.
- [11] E. Witten, Nucl. Phys. B156 (1979) 269.
G. Veneziano, Nucl. Phys. B159 (1979) 213.
- [12] D. Diakonov, M. Polyakov and C. Weiss, Nucl. Phys. B461 (1996) 539 (hep-ph/9510232).
- [13] T. Schäfer, Phys. Rev. D66 (2002) 076009 (hep-ph/0206062).
- [14] E. Witten, Nucl. Phys. B149 (1979) 285.
- [15] M. Teper, Z. Phys. C5 (1980) 233.
- [16] H. Neuberger, Phys. Lett. B94 (1980) 199.
- [17] D. Gross, R. Pisarski and L. Yaffe, Rev. Mod. Phys. 53 (1981) 43.
- [18] M. Teper, Nucl. Phys. Proc. Suppl. 83 (2000) 146 (hep-lat/9909124).
- [19] N. Cundy, M. Teper and U. Wenger, hep-lat/0309011, hep-lat/0309170 and in preparation.
- [20] D. Smith and M. Teper, Phys. Rev. D58 (1998) 014505 (hep-lat/9801008).
- [21] G. 't Hooft, in *Large N QCD* (Ed. R.F. Lebed, World Scientific 2002) (hep-th/0204069).
- [22] J. Hoek, M. Teper and J. Waterhouse, Phys. Lett. B180 (1986) 112; Nucl. Phys. B288 (1987) 589.
M. Teper, Phys. Lett. B202 (1988) 553.
- [23] M. Teper, Phys. Lett. B171 (1986) 81.

N	β	$\beta_c(aT_c = 0.2)$	lattice	$a\sqrt{\sigma}$	$\langle Q_I^2 \rangle$	$\langle Q_r^2 \rangle$
2	2.3715	2.3714(6)	12^4	0.2879(13)	3.69(13)	3.39(12)
3	5.8000	5.8000(5)	10^4	0.3133(13)	2.917(79)	2.469(74)
4	10.637	10.637(1)	10^4	0.3254(14)	3.375(90)	2.881(81)
6	24.515	24.514(3)	10^4	0.3385(15)	3.48(18)	2.96(17)
8	44.000	43.98(3)	10^4	0.3413(13)	3.20(42)	2.68(35)

Table 1: Fluctuation of the topological charge in various $SU(N)$ lattice gauge theories for a fixed value of the lattice spacing $a = 1/5T_c$. Q_r is the raw real-valued lattice charge and Q_I is our best estimate of the integer that corresponds to it. Also shown is the string tension, σ , the critical value of β , and the lattice parameters.

N	β	$\chi_{I,t}^{1/4}/\sqrt{\sigma}$	$\chi_{r,t}^{1/4}/\sqrt{\sigma}$
2	2.3715	0.4013(40)	0.3928(40)
3	5.8000	0.4171(34)	0.4001(35)
4	10.637	0.4165(33)	0.4004(33)
6	24.515	0.4034(56)	0.3875(58)
8	44.000	0.392(13)	0.375(13)

Table 2: The topological susceptibility in units of the string tension for the calculations in Table 1.

N	β	lattice	$a\sqrt{\sigma}$	T/T_c	$\chi_{r,t}/\sigma^2$		
					confined	deconfined	$T = 0$
3	5.8000	$32^3 5$	0.3133(13)	1.00	0.0270(13)*	0.0141(13)*	0.0256(9)
4	10.635	$32^3 5$	0.3262(15)	1.00	0.0260(19)	0.0070(7)	0.0257(9)
6	24.515	$16^3 5$	0.3385(15)	1.00	0.0199(14)	0.00171(14)	0.0226(13)
8	43.965	$12^3 5$	0.3462(15)	0.995	0.0161(28)	0.00005(3)	0.0198(26)

Table 3: Topological susceptibility in units of the string tension calculated separately in the confined and deconfined phases, for the values of N , on the lattice volumes and at the values of β shown.

$SU(8)$					
β	lattice	$a\sqrt{\sigma}$	T/T_c	$\chi_{r,t}/\sigma^2$:conf	$\chi_{r,t}/\sigma^2$:deconf
44.00	$8^3 4$	0.3413(13)	1.26		0.00000(4)
43.85	8^4	0.3630(21)	0	0.0191(24)	

Table 4: Some additional $SU(8)$ calculations of the topological susceptibility in units of the string tension.

$SU(6)$					
β	lattice	$a\sqrt{\sigma}$	T/T_c	$\chi_{r,t}/\sigma^2$:conf	$\chi_{r,t}/\sigma^2$:deconf
24.500	$16^3 5$	0.3414(20)	0.99		0.00219(18)
24.530	$16^3 5$	0.3356(20)	1.01		0.00115(10)
24.515	$10^3 4$	0.3385(15)	1.25		0.000012(5)

Table 5: Some additional $SU(6)$ calculations of the topological susceptibility in units of the string tension.

$SU(4)$					
β	lattice	$a\sqrt{\sigma}$	T/T_c	$\chi_{r,t}/\sigma^2$:conf	$\chi_{r,t}/\sigma^2$:deconf
10.645	$12^3 5$	0.3222(16)	1.01		0.0058(3)*
10.642	$20^3 5$	0.3235(16)	1.01		0.0060(3)
10.637	$20^3 5$	0.3254(14)	1.00	0.0246(10)*	0.0071(4)*
10.635	$20^3 5$	0.3262(16)	1.00	0.0247(11)*	0.0076(4)*
10.633	$20^3 5$	0.3270(16)	1.00	0.0257(8)*	0.0074(5)*
10.637	$12^3 4$	0.3254(14)	1.00		0.000115(22)

Table 6: Some additional $SU(4)$ calculations of the topological susceptibility in units of the string tension.

$SU(3)$					
β	lattice	$a\sqrt{\sigma}$	T/T_c	$\chi_{r,t}/\sigma^2$:conf	$\chi_{r,t}/\sigma^2$:deconf
5.7950	$20^3 5$	0.3163(20)	0.99	0.0243(10)	
5.7975	$20^3 5$	0.3148(16)	1.00	0.0253(8)*	0.0144(10)*
5.8000	$20^3 5$	0.3133(13)	1.00		0.0132(5)
5.8025	$20^3 5$	0.3118(16)	1.00		0.0124(5)
5.8000	$12^3 4$	0.3133(13)	1.25		0.00042(4)

Table 7: Some additional $SU(3)$ calculations of the topological susceptibility in units of the string tension.

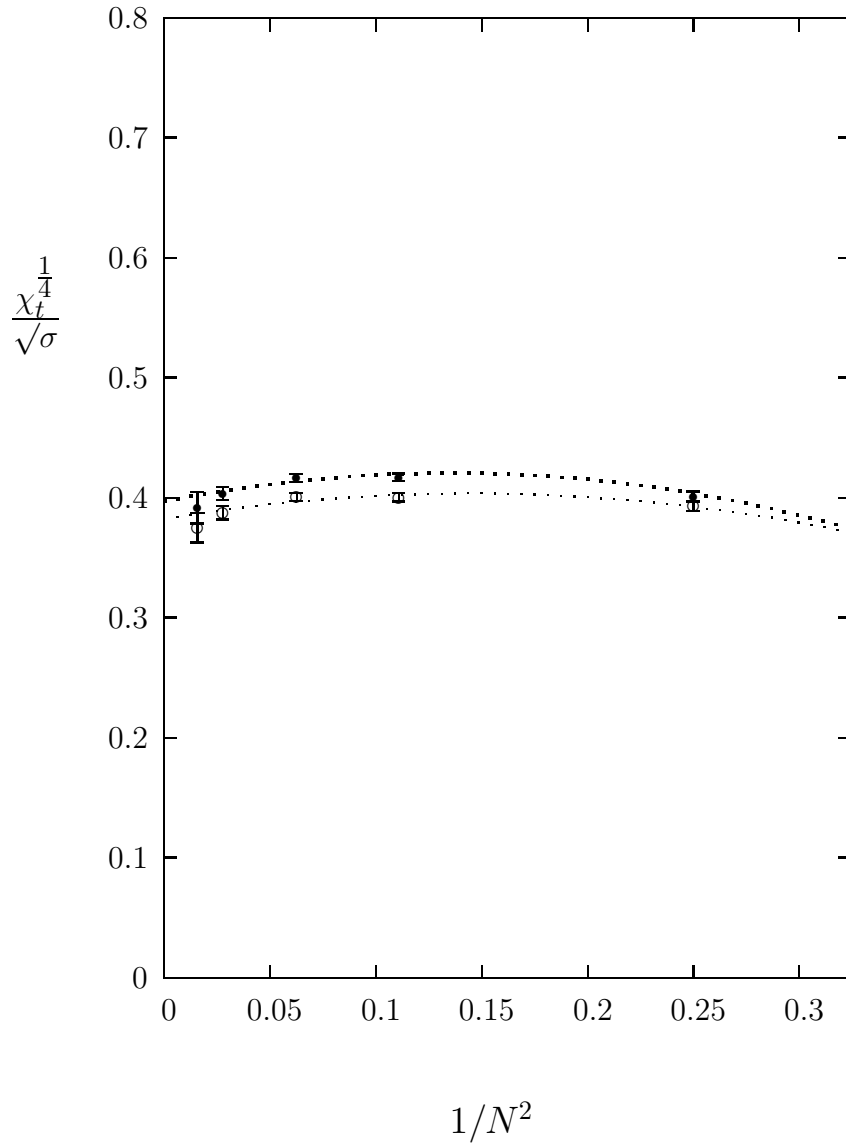


Figure 1: The topological susceptibility, χ_t , in units of the string tension, σ , plotted versus $1/N^2$. The calculations are performed at a fixed lattice spacing $a \simeq 1/5T_c$. The line is a large- N extrapolation that includes $O(1/N^2)$ and $O(1/N^4)$ corrections.

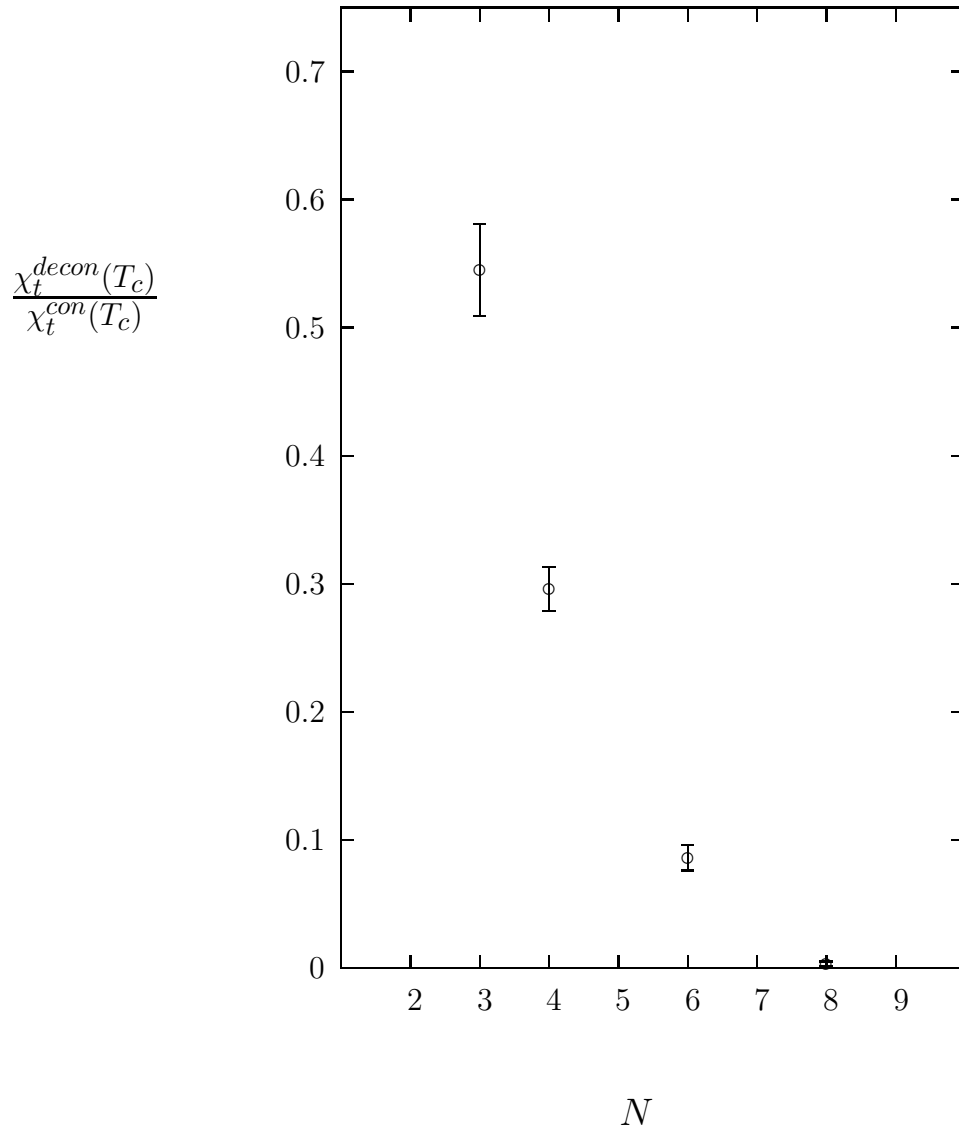


Figure 2: The ratio of the topological susceptibility, χ_t , in the deconfined and confined phases at $T \simeq T_c$.

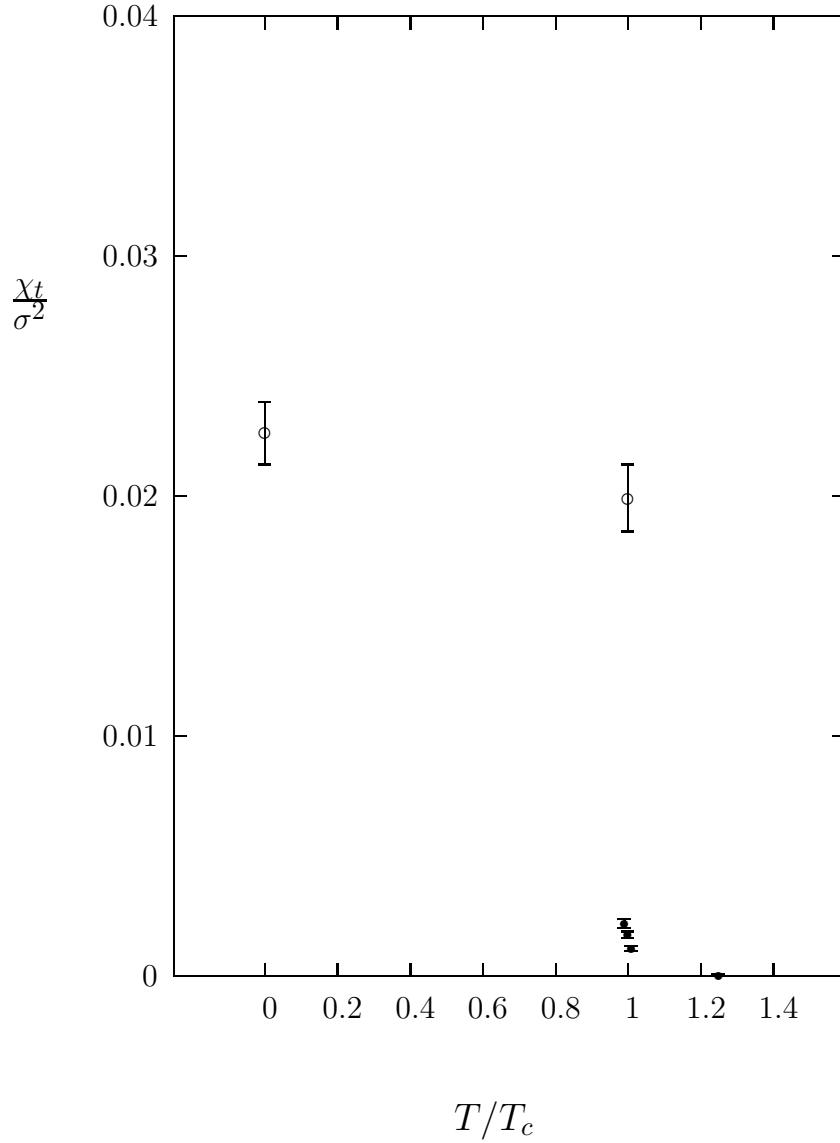


Figure 3: The topological susceptibility, χ_t , in units of the string tension, σ , plotted versus T/T_c for $SU(6)$, plotted separately for the confined, \circ , and deconfined, \bullet , phases. The calculations are performed at a lattice spacing $a \simeq 1/5T_c$.

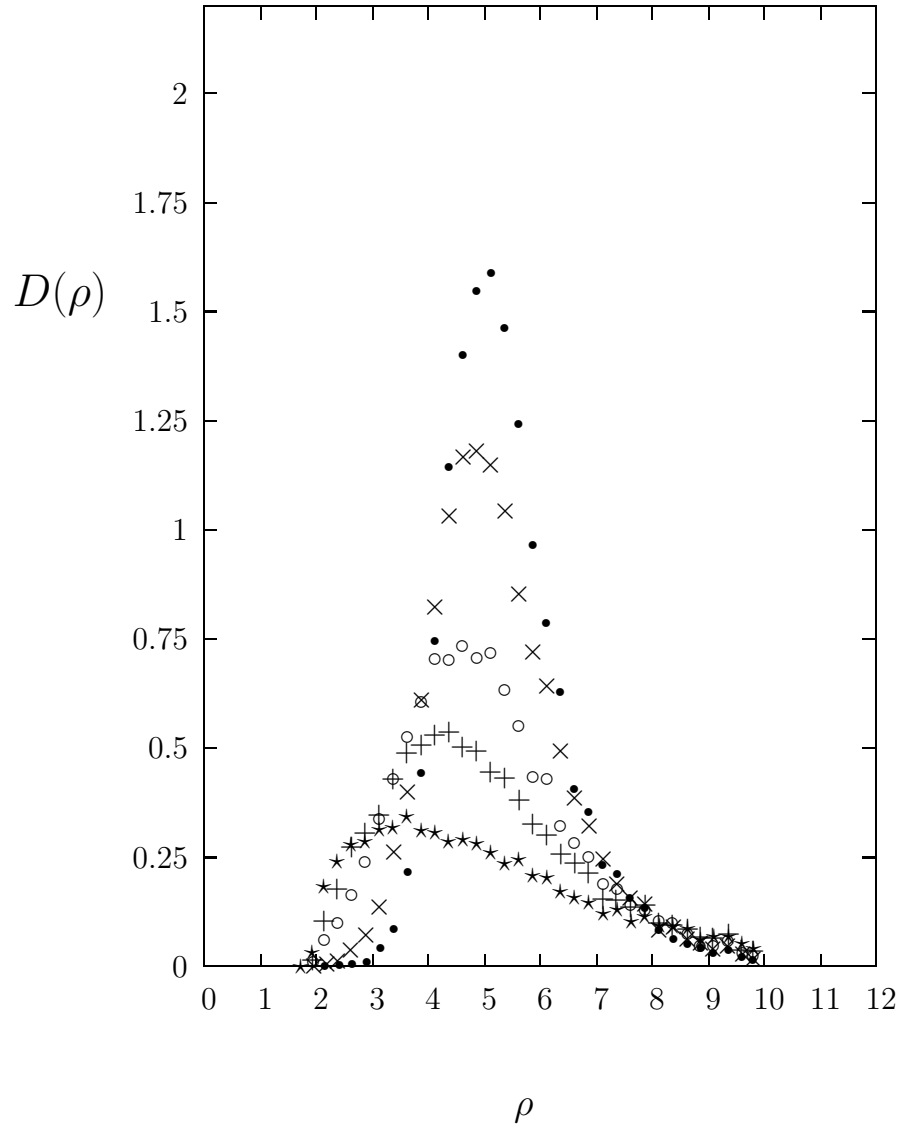


Figure 4: The instanton size density, $D(\rho)$, for $N = 2(\star), 3(+), 4(\circ), 6(\times), 8(\bullet)$ on (mostly) 10^4 lattices with $a = 1/5T_c$.

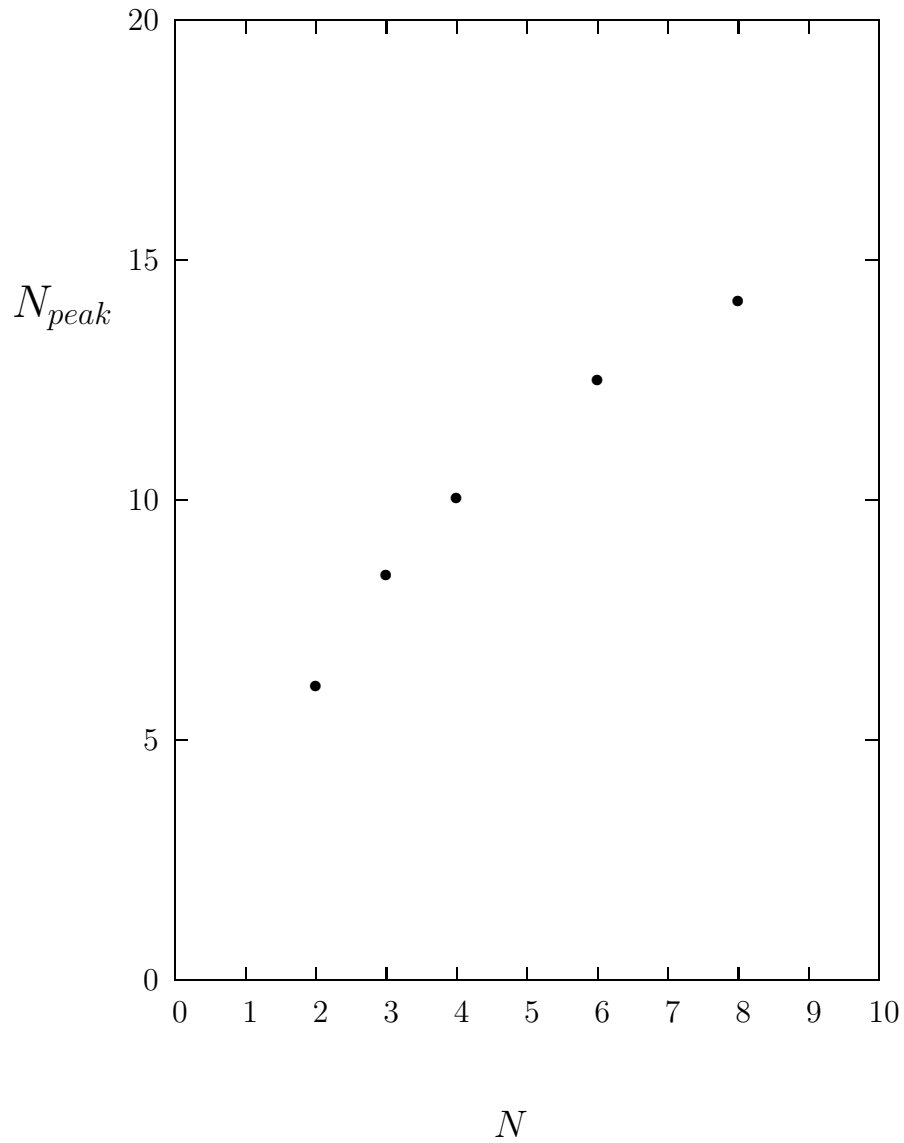


Figure 5: The average number of instantons versus N at $a = 1/5T_c$ on a 10^4 volume, from the calculations listed in Table 1

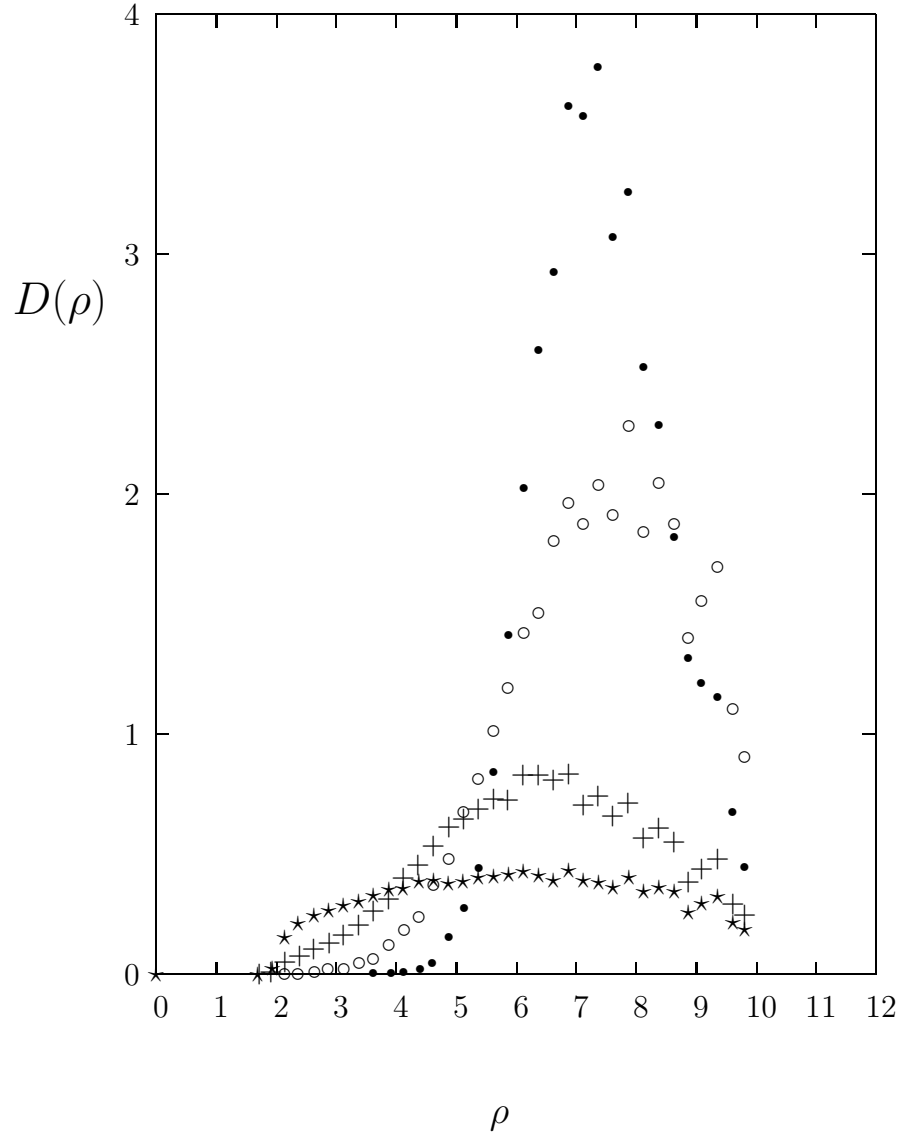


Figure 6: The instanton size density, $D(\rho)$, for $N = 2(\star), 3(+), 4(\circ), 8(\bullet)$ on 16^4 lattices with $a \simeq 1/8T_c$.

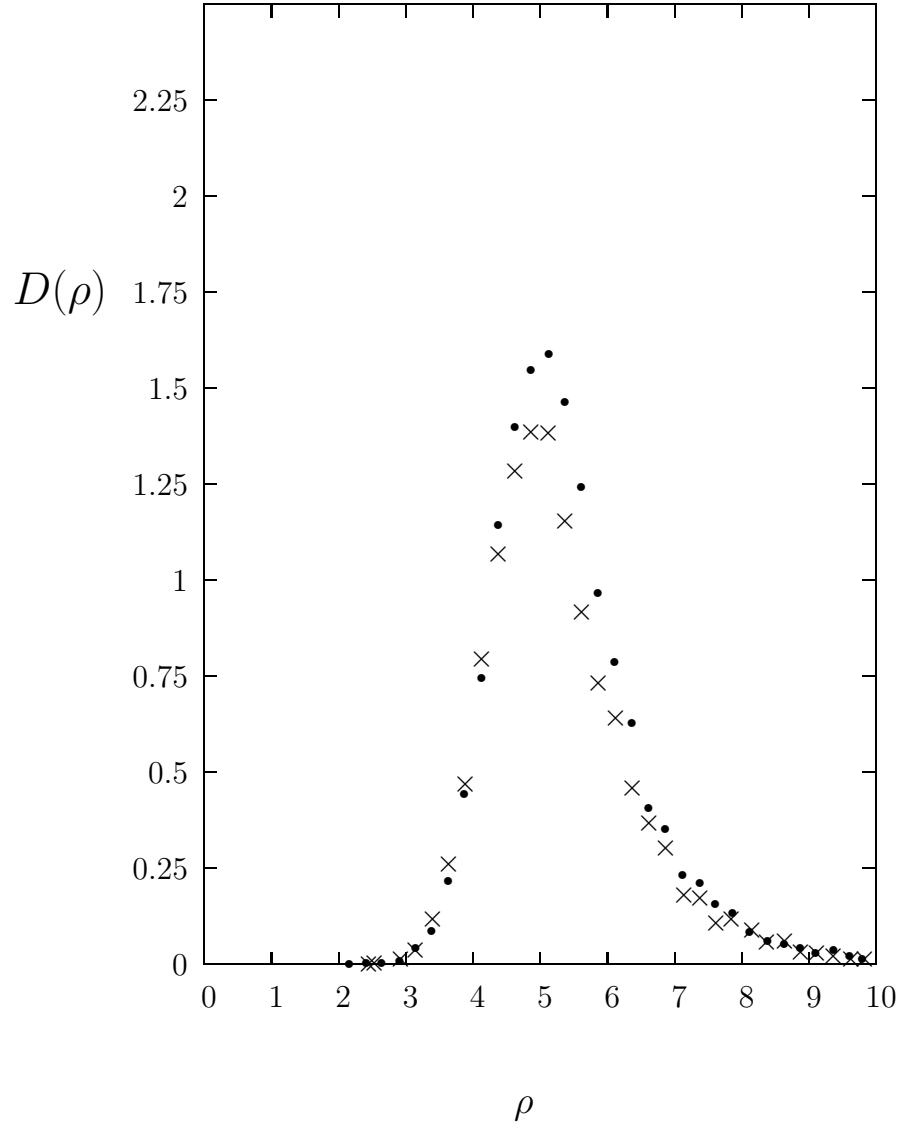


Figure 7: The $SU(8)$ instanton size density, $D(\rho)$, at $T \simeq 0$ (●) and at $T \simeq T_c$ (×) in the confined phase, with $a \simeq 1/5T_c$ in both cases. Normalised to a 10^4 volume.

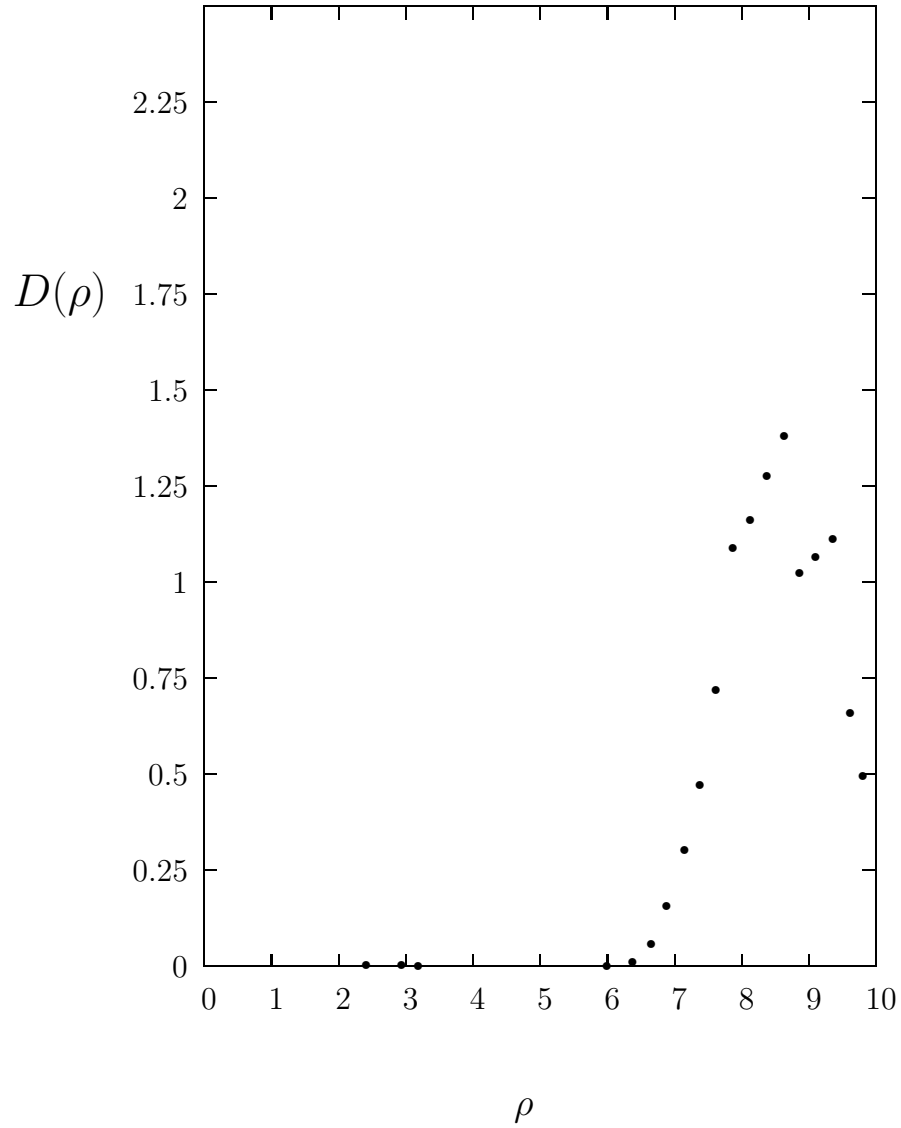


Figure 8: The $SU(8)$ instanton size density, $D(\rho)$, at $T \simeq T_c$ in the deconfined phase, with $a \simeq 1/5T_c$. Normalised to a 10^4 volume.

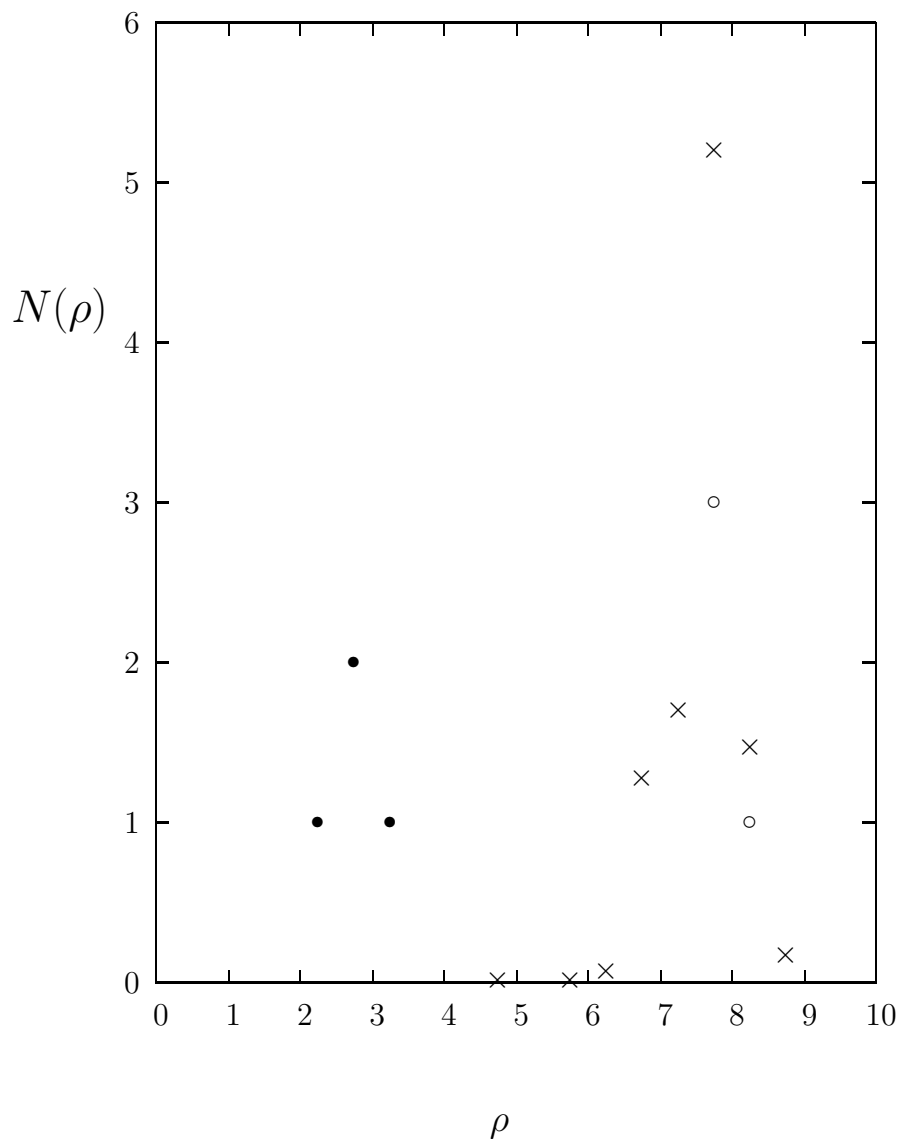


Figure 9: The number of instantons in 500 lattice fields using only the largest positive and negative peaks in each field. All in the deconfined phase, at $T = T_c$, on a 12^{35} lattice in $SU(8)$. Separately for the 4 configurations with $Q \neq 0$ and for the 496 lattice fields with $Q = 0$. The latter (\times) have been divided by 100 so as to fit on the same plot. For the former we show separately sizes from peaks with the same sign as Q (\bullet) and with the opposite sign (\circ).

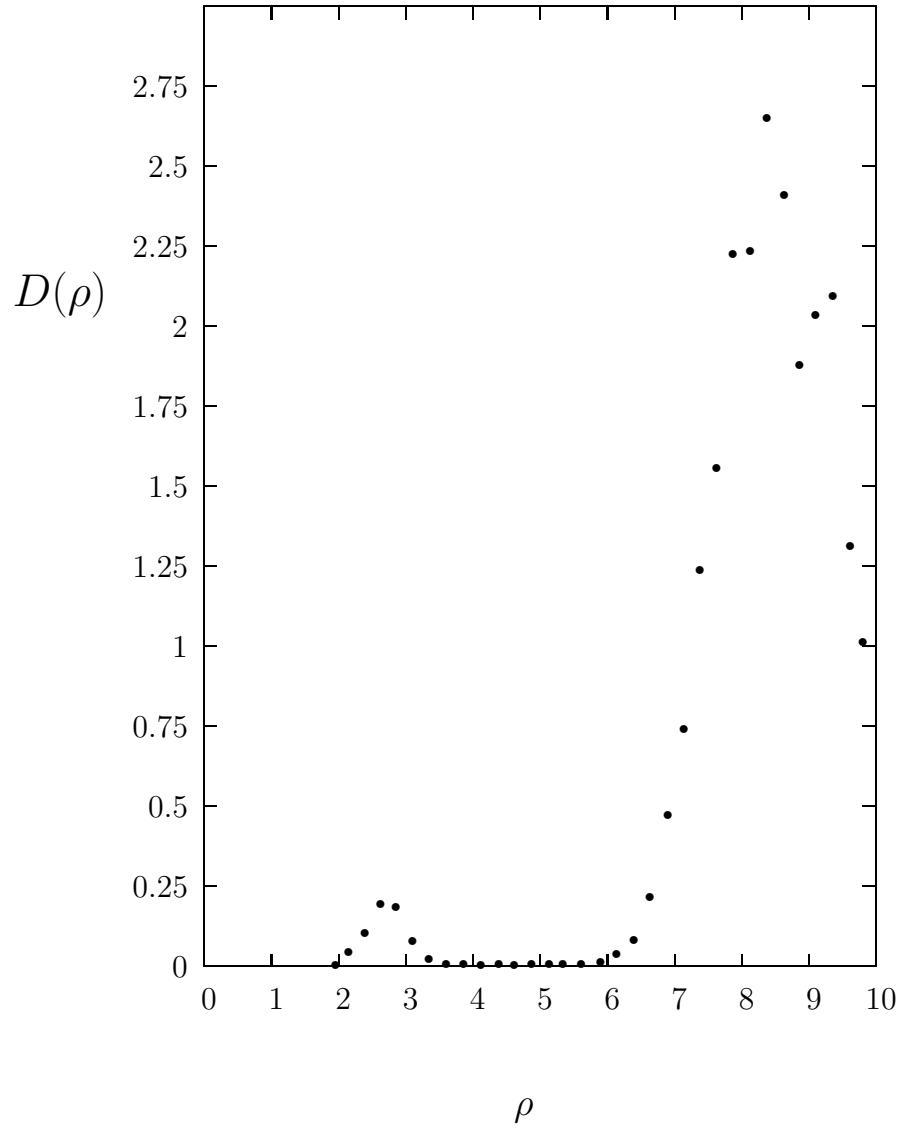


Figure 10: The $SU(6)$ instanton size density, $D(\rho)$, at $T \simeq T_c$ in the deconfined phase, with $a \simeq 1/5T_c$. Normalised to a 16^{35} volume.

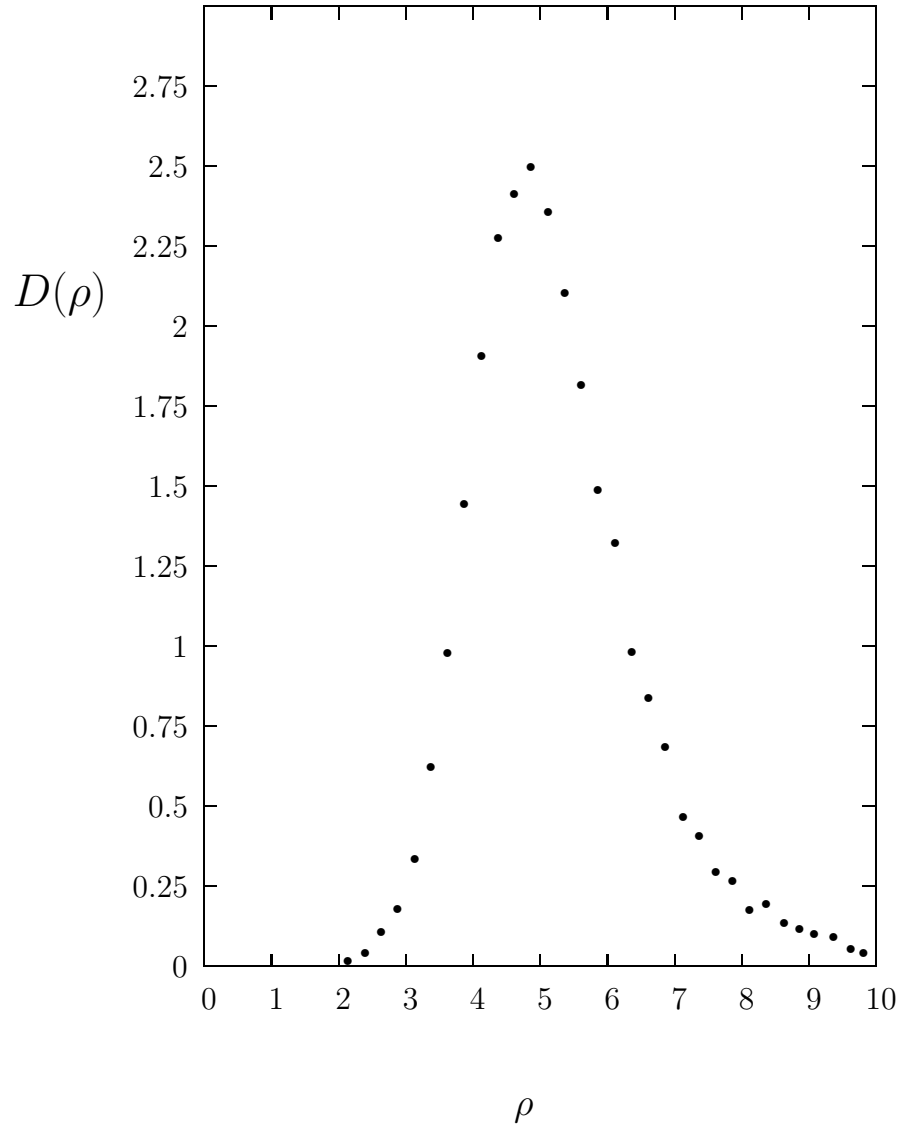


Figure 11: The $SU(6)$ instanton size density, $D(\rho)$, at $T \simeq T_c$ in the confined phase, with $a \simeq 1/5T_c$. Normalised to a 16^{35} volume.

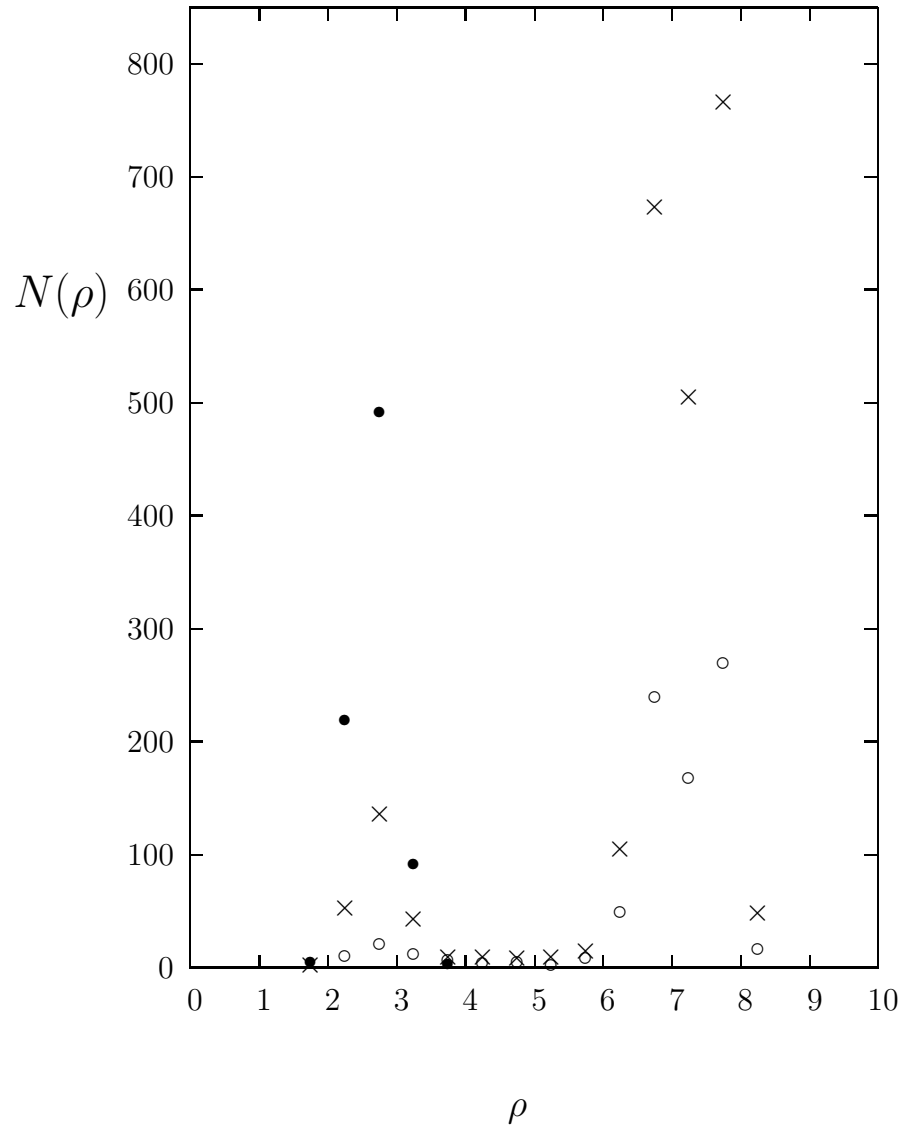


Figure 12: The number of instantons in 2000 lattice fields using only the largest positive and negative peaks in each field. All in the deconfined phase, at $T = T_c$, on a 16^{35} lattice in $SU(6)$. Separately for the lattice fields with $Q \neq 0$ and for the fields with $Q = 0$, \times . For the former we show separately sizes from peaks with the same sign as Q (\bullet) and with the opposite sign (\circ).

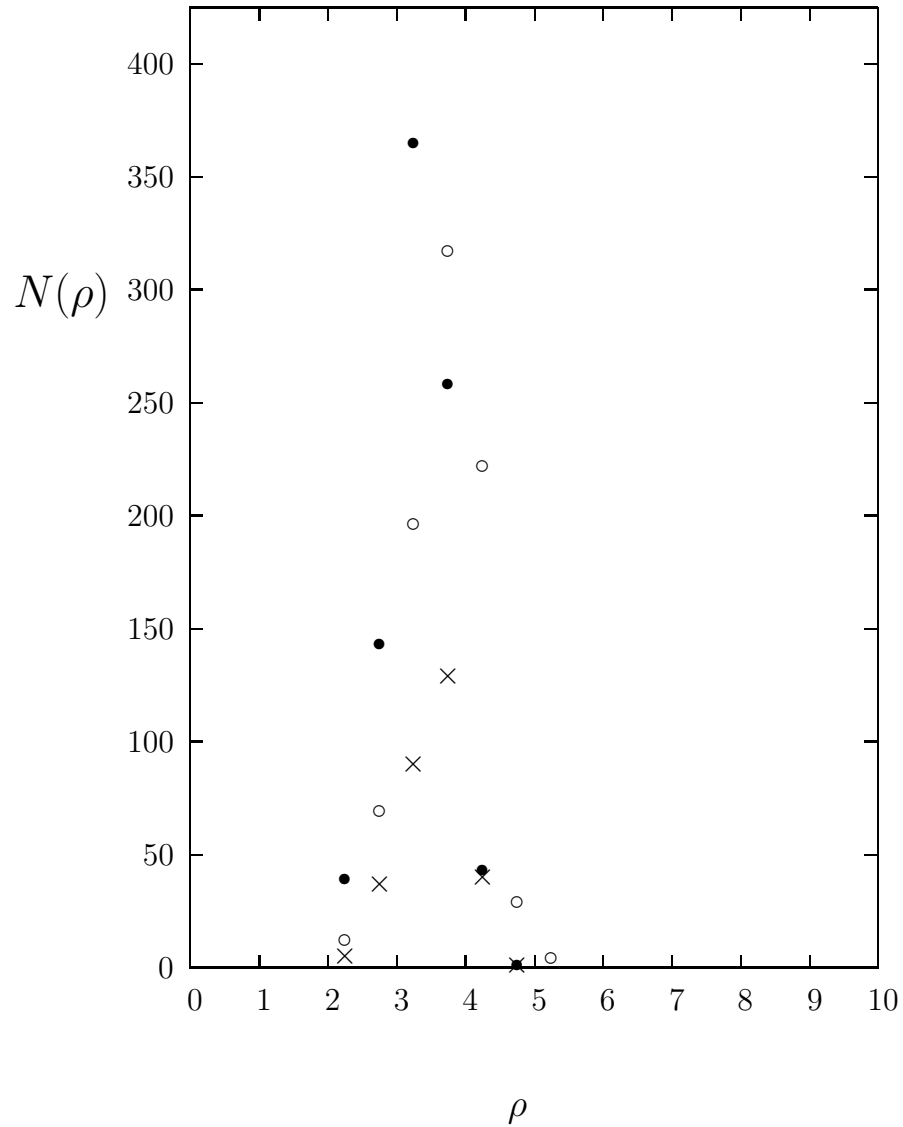


Figure 13: The number of instantons in 1000 lattice fields using only the largest positive and negative peaks in each field. All in the confined phase, at $T = T_c$, on a $16^3 5$ lattice in $SU(6)$. Separately for the lattice fields with $Q \neq 0$ and for the fields with $Q = 0$, \times . For the former we show separately sizes from peaks with the same sign as Q (•) and with the opposite sign (○).